# Textural pattern of secondary gypsum in the Basal Anhydrite of the Asmari Formation, SW Iran

**Behrouz Rafiei\*, Saeideh Rahmani**

[1] *Department of Geology, University College of Sciences, University of Bu-Ali sina, Hamedan, Iran*
*\*Corresponding author, e-mail: b_rafiei@basu.ac.ir*

## Abstract

The Oligocene–Miocene deposits of the Asmari Formation are located in SW of the Zagros Mountains of Iran. The lower part of the Asmari Formation consists of an evaporite bed that is termed Basal Anhydrite. Seven sections from four different anticlines were selected and sampled for petrographic and mineralogical analyses .The petrographical examinations were carried out using an optical polarized light microscope and SEM analyses. To determine the mineralogical composition, evaporite samples were analyzed by X-Ray Diffraction. Particular petrographic characteristics, at the macro- and microscales, especially common pseudomorphic features and mineralogical analysis of the Basal Anhydrite showed that anhydrite was transformed to gypsum during exhumation. Diagenetic processes caused an increase in the pure gypsum and a simultaneous decrease in the residual anhydrite. Two main textures, fine-crystalline (alabastrine) and coarse crystalline (porphyroblast), were distinguished in samples indicating replacement of anhydrite by gypsum. The textures related to the tectonic movements in evaporite rocks were observed in the thin sections. The effect of tectonic varies due to the type of gypsum texture. Microcrystalline gypsum is mostly recrystallized to form coarse-crystalline and aligned-flowing texture. Coarse crystalline gypsum which contains anhydrite is more resistant against the tectonic effects because it shows only a little rotation.

**Keywords**: *Basal Anhydrite, Asmari Fm., Evaporite, Secondary Texture, Dezful Embayment*

## Introduction

Gypsum ($CaSO_4.2H_2O$) and anhydrite ($CaSO_4$) are two kinds of calcium sulphate. Despite anhydrite, gypsum is the most abundant calcium sulfate mineral that is formed under normal sedimentary conditions while anhydrite is rarely formed on the surface, but only in arid and hot supratidal environments (sabkha) in the presence of concentrated brines (Kinsman, 1966; Shearman, 1985; Testa & Lugli, 2000). During uplifting of anhydrite, it goes back to gypsum (Testa & Lugli, 2000), in other words, gypsum is created by rehydration of the anhydrite. Secondary gypsums are usually restricted to within a few hundred feet from the surface, but locally occur at depths of several thousand feet (Murray, 1964; Holliday, 1970). Most ancient evaporites, especially gypsum and anhydrite, show evidence of secondary or diagenetic textures.

The processes of secondary evaporite formation indicate the displace growth, recrystallization, back reactions and replacement that are reflected in crystals and textures (Warren, 2007; Warren, 2016).

The petrography and diagenetic relationship between gypsum and anhydrite in these locations constitutes an excellent opportunity to better understanding the post-depositional processes that took place after primary evaporite formation. This paper describes the petrographic properties of the Basal Anhydrite, Asmari Fm., and tectonic

influence on its textures. The same tectonic activity results in different textures in gypsum, so that some of them have been recrystallized and others have shown a little rotation.

The Basal Anhydrite is located in the lower part of Asmari Formation. Lithologically, the Asmari Formation mainly consists of limestone, dolomitic limestone with minor marl/shale and evaporates (Motiei, 1993). Ehrenberg *et al.* (2007) considered the Basal Anhydrite as a type of primary anhydrite, which has been established in the deep basin at the time of retrogression. In fact, the Basal Anhydrite is composed of anhydrite in subsurface and gypsum in outcrops.

The Basal Anhydride has always been considered along with the Asmari Formation and Kalhur Member. Petrographical characteristics of the Basal Anhydrite have not been studied yet.

The important aspects of the present paper are: (1) Conversion of anhydrite to gypsum throughout outcrops; (2) identification and interpretation of secondary gypsum textures in the study areas, and (3) the influence of tectonic activities on the secondary textures.

## Geographical and Geological setting

The Oligocene-Miocene age Asmari Formation is a carbonate succession in the various parts of Zagros

basin, southwest Iran, which is dominated in the Dezful Embayment Zone (Fig. 1).The Basal Anhydrite at the base of the Asmari Formation is observed in the Dezful Embayment Zone and the Izeh Zone where facies associations of the Asmari Formation are varied between Bangestan and Kuh-e-Safid anticline. The Dezful Embayment is one of structural zones in the study area, which is surrounded by Mountain Front, Balarud and Kazerun faults (Fig. 2). Most of the oil fields are located in this zone (Cenozoic and Mesozoic).

The Ahwaz sandstone and Kalhur evaporites are members of the Asmari Formation (James and Wynd, 1965). The Kalhur Member is equal to the Lower-Middle Asmari (Motiei, 1993).

Basal Anhydrite shows similarities in shape and size with lower part of the Kalhur Member. Strontium isotope stratigraphy of the Kalhur Member and the Basal Anhydrite in the Dezful Embayment indicate Aquitanian age (Ehrenberg *et al.,* 2007; van Buchem *et al.,* 2010), when the basin was isolated from the open sea (James and Wynd, 1965; Adams and Bourgeois, 1967; Adams, 1969; Kavoosi & Sherkati, 2012; Daraei *et al.,* 2014). Thickness and lateral extending of the Basal Anhydrite reveal that it was submarine sediments which formed in isolated saltern basins (Kavoosi & Sherkati, 2010).
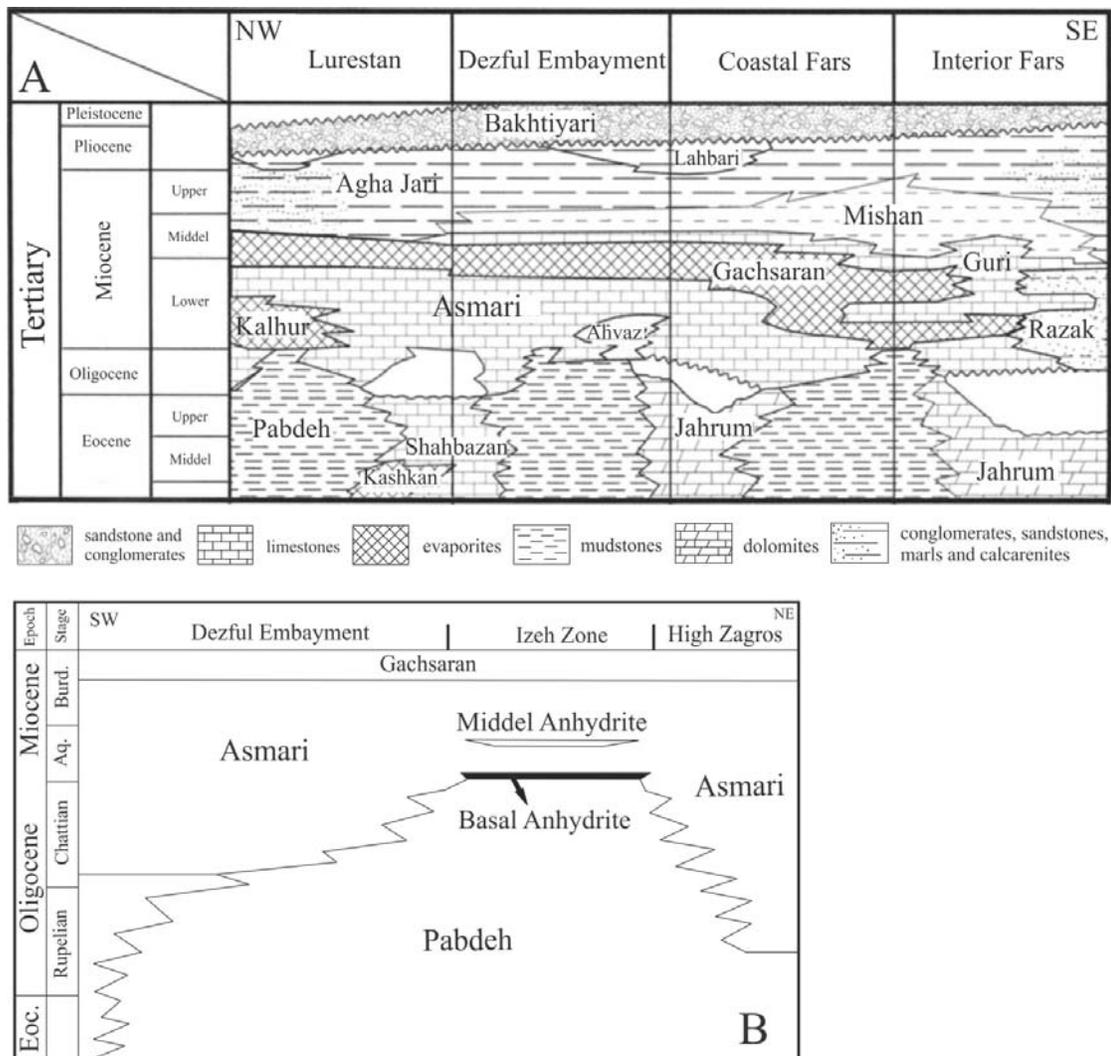


Figure 1. Lithostratigraphic scheme. A: Correlation chart of the tertiary of southwest Iran (modified from Ala 1982 and Motiei 2001). B: Schematic presentation of the main lithostratigraphic units encountered in the study area along a southeast to northwest transects (Van Buchem *et al.,* 2010).
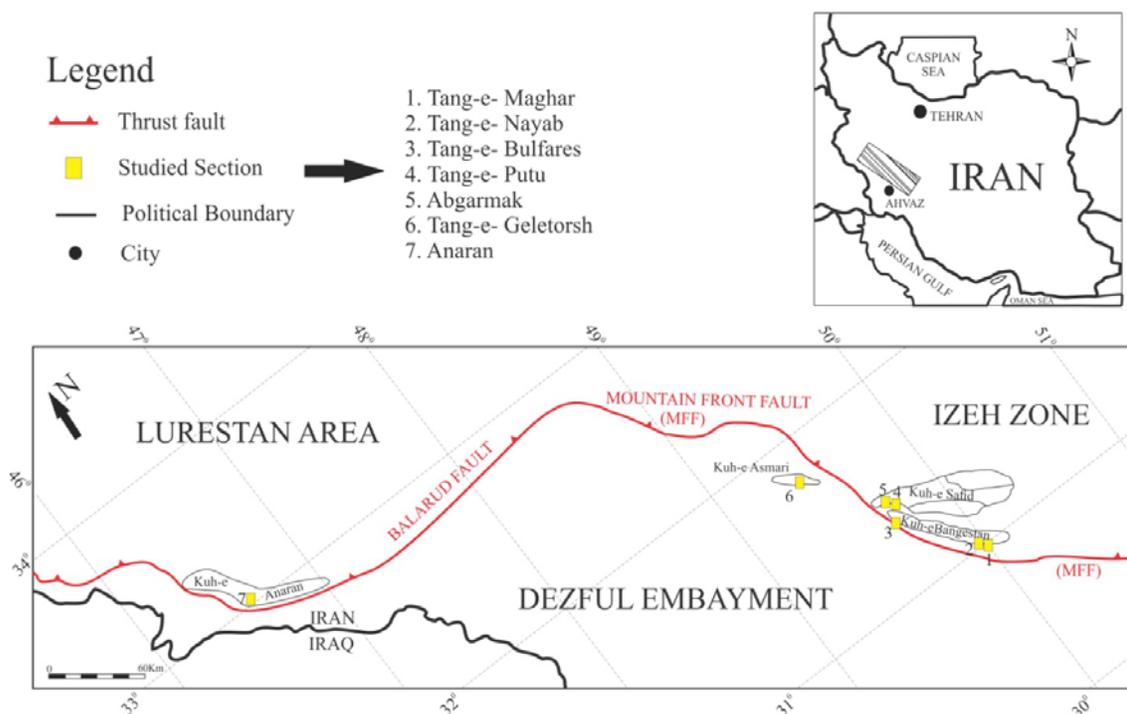
Figure 2. Location map of the study areas in southwest Iran. The locations of the seven outcrops are indicated. Shaded box shows the location of the study area.

According to the morphology of the basin, the anhydrite has been precipitated in depth of 10-15m (Van Buchem *et al*., 2010).

To investigate the petrographical characteristics of Basal Anhydrite and lower part of Kalhur member, and due to the unavailability of data from subsurface, Basal Anhydrite was selected in different structural zones (zone izeh, Dezful Embayment, Lurestan area), type sections of the Asmari Fm. (Tang-e- Geltorsh Section) and the Kalhur Member (Anaran Section). Generally, Basal Anhydrite was studied in seven outcrops at four different anticlines, including the Kuh-e- Bangestan (Tang-e- Maqar; Tang-e- Nayab and Tang-e- Bulfares Sections), Kuh-e- Safid (Tang-e- Putu and Abgarmak Sections), Kuh-e- Asmari (Tang-e- Geltorsh Section) and Kuh-e- Anaran (Anaran Section) (Fig. 2). At these sections, the Basal Anhydrite overlies on the Pabdeh Formation (or Stromatolitic Boundstone) and is overlain by the Asmari Formation, with discontinuous but conformable contact.

**Methods**
This paper was accomplished based on the field study (macro-scale) and petrographic examinations (micro-scales).The thickness of Basal Anhydrite in

Putu, Bulfares, Nayab, Abgarmak, Anaran, Geletorsh and Maqar sections are 15m, 12m, 12m, 10m, 7m, 7m and 4m respectively (Fig. 3). There are no significant changes in the appearance characteristics of it. Systematic sampling was carried out whit interval of half meter. One hundred thirty-four evaporite samples were collected from the Basal Anhydrite in the study area. Sixty seven samples were selected from different sections for petrographical studies. The petrographical examinations were carried out using an optical polarized light microscope and SEM analyses.
The crystal fabrics and textures were mainly described according to Ortí *et al.* (2010) and Warren (2016).

Based on petrographic studies and in order to more accurate assessment of the crystalline textures in gypsum samples, three different samples were studied through SEM analysis (Jeol Scanning Microscope-840). To determine the mineralogical composition, twenty-one evaporite samples including three samples from each seven sections were analyzed by the diffraction patterns were gathered with Italstructures diffractometer using Cu kα radiation (40 kV, 30 mA). The standard 2θ scan range was taken to be 2–70˚. The XRD and SEM analyses were done at Bu-Ali Sina University.
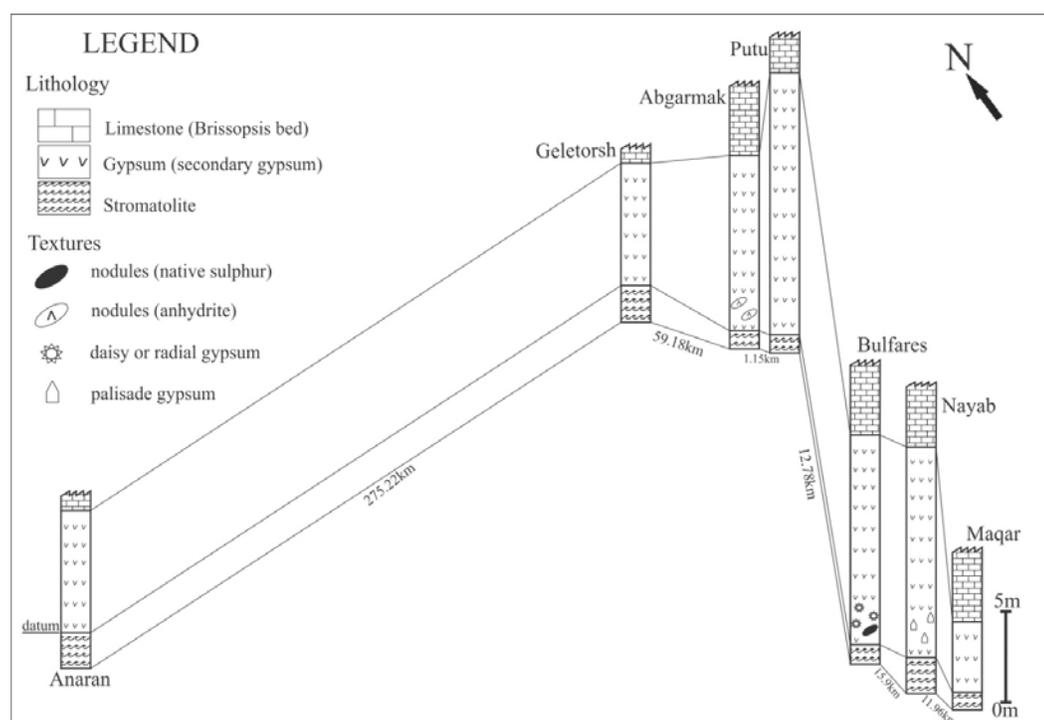
Figure 3. Correlation of the stratigraphic sections studied in the Basal Anhydrite in the Asmari Formation. The location of these sections is indicated in Figure 2. The datum is lowermost gypsum at the base of the Basal Anhydrite.

## Result and Discussion

Based on field studies, the Basal Anhydrite is underlain by Brissopsis bearing Beds and overlain on the Stromatolitic Boundstone (Fig. 4). Their facial characteristics and relationships with anhydrite are as follow:

*Stromatolitic Boundstone:* This part is located at the base of the Basal Anhydrite that its thickness changes between 1 and 2 m (Fig. 4A). Presence of the stromatolite suggests either a subaqueous origin or at sea level fall to near exposure of these facies (van Buchem et al., 2010).

*Brissopsis bearing Beds:* this carbonate facies contains *Zeauvigerina* spp., *Haplophragmium Slingeri*, *Ditrupa* spp., *Genus 2*. sp1 and *Small Globigerina* that correspond to Aquitanian age (James and Wynd, 1965; Adams and Bourgeois, 1967; Adams, 1969). This part lies over the Basal Anhydrite (Fig. 4B). In the most recent classification of Asmari Formation, these beds are defined in this Formation (van Buchem et al., 2010; Rahmani et al., 2012).

*Basal Anhydrite:* this unit has lensoidal form due to elastic properties of evaporites and tectonic activity of the studied area.

In terms of mineralogy the anhydrite unit is composed of calcium sulphate that is weathered and mainly altered in outcrops. In the study area, they are composed of gypsum (secondary, primary, diagenetic) and minor quantities of anhydrite. Other associated minerals are celestite ($SrSO_4$) and scarce native sulphur which are as follow:

*Primary gypsum*
Primary evaporite minerals directly precipitate from brines and preserve the original texture and have not any anhydrite relics (Ingerson, 1968; Dronkert, 1985).They are present at the margin of the outcrop in the Nayab Section.

*Secondary gypsum*
This kind of gypsum has been formed due to the replacement of a precursor anhydrite or has been occurred during diagenesis. It is necessary to mention that the conversion of anhydrite to gypsum can be regarded as a form of retrogressive metamorphism (Holiday, 1970). Diagenetic gypsum is precipitated from fluids of dissolved evaporates. Therefore, it does not represent morphologies inherited from precursor anhydrite and absence of anhydrite relics (Ortí & Rosell, 2000).
Crystal size in the primary gypsum is varied from few centimeters to several meters, while gypsum observed in all studied sections are fine-grained and

have sucrosic texture. This gypsum called Alabaster. It is the other form of telogenetic gypsum and anhydrite pervasively rewaters to gypsum. Presence of gypsum in outcrops is also confirmed by the results of XRD analysis on 21 samples (Fig. 5).

*Anhydrite*

In the Dezful Embayment structural zone, anhydrite is present in the subsurface, confirmed by data gathered from borehole logs (van Buchem *et al.,* 2010). Nodular anhydrite was telogenetically rehydrated to gypsum which may be retained remnants of the actual primary anhydrite as nodular anhydrite encased in secondary gypsum (Warren, 2016). Pure nodular anhydrite is scarce. It is observed only in the Abgarmak Section where the layers are inverted by tectonic process. Anhydrite relics present in all thin sections due to conversion of anhydrite to gypsum.

*Celestite*

Celestite is a common mineral of gypsiferous rocks (Playá & Rosell, 2005). Anhydrite and gypsum can be replaced by celestite (Carlson, 1987). When secondary gypsum is formed during hydration of anhydrite, not all of the strontium in the anhydrite lattice enter the gypsum lattice, and precipitates as celestite instead (Holliday, 1970; Dean, 1978).

The celestite is observed as veins, lenses and layers near the Basal Anhydrite. Celestite was nearly found in all sections but the highest amount is in the Bulfares Section.

*Native sulphur*

Most of the native sulphurs are microbially produced from calcium sulphate (sulphate reduction) of anhydrite and gypsum in a sedimentary basin (holster, 1992, Warren, 2016).
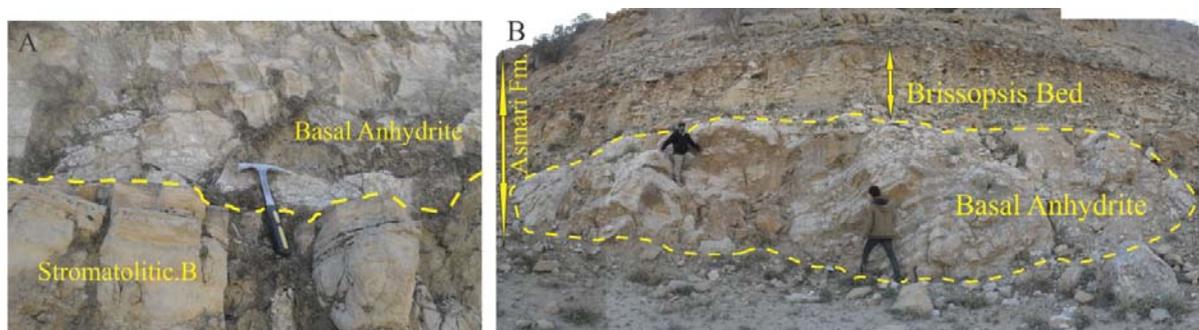


Figure 4. Basal Anhydrite outcrop section: A) Stromatolitic Boundstone of the base of the Basal Anhydrite at Bulfares outcrop section (Hammer length: 30 cm.). B) Tang-e-Maqar Section: overview of the Basal Anhydrite with the lower part of the Asmari Formation limestones (Brissopsis Bed). The Basal Anhydrite interbedded in the limestones of the Asmari Formation.
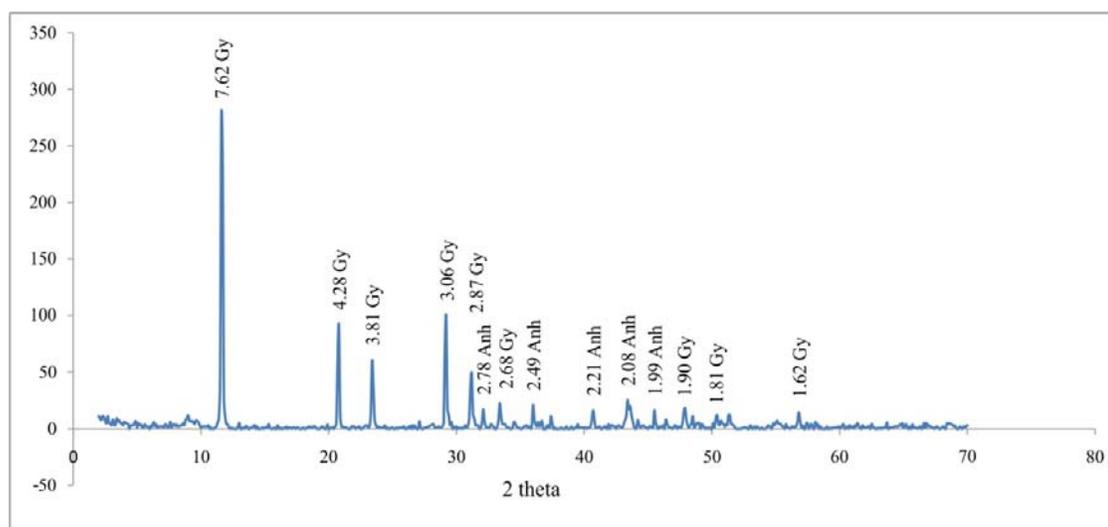


Figure 5. X-ray diffraction patterns of secondary gypsum from with minor anhydrite content from the Tang-e- Geltorsh Section. Gy: gypsum; Anh: anhydrite.

The presence of patches of native sulphur within the gypsum can be assumed as the sign of rehydrated anhydrite (Aref, 1998b). Diagenetic sulphur mineral or native sulphur is observed in Bulfares Section. This is a form of evaporite-related deposit and exists as patches in the secondary gypsum.

*Textural pattern:*
*Macroscopic texture (gypsum fabrics)*
Rehydration fabrics were observed in the field study. They include alabastrine gypsum (fine grained), Porphyroblastic gypsum (palisade, daisy) and fibrous gypsum (satin-spar) (Holliday, 1970; Warren et al., 1990; Warren, 1999; Arzaghi *et al.,* 2012; Ortí *et al.,* 2012). Nodular texture is also present in the study area.

The fabric of gypsum unit is mainly fine-grained (alabastrine). It is created where precursor anhydrite rehydrate to gypsum. This process is occurred in the zone of active phreatic flow (Warren, 2016).

The length of palisade gypsum ranges from 7 cm to 10 cm and is formed at the margin of the outcrop in the Nayab Section. Crystals have a characteristic growth-aligned gypsum texture (Fig. 6A). It seems that they grew upwards from the bottom in crystallographic continuity (Bąbel, 2007) and at a depth of no more than a few meters (Bąbel, 2004a). The daisy gypsum is formed from fibrous crystals which arrange into a radial pattern with the average 22 cm in diameter (Fig. 6B). This gypsum is formed under rather homogenous conditions when massive nodular anhydrite unit entering the lowermost parts of the telogenetic zone (Warren, 2016). This type of gypsum is only observed in the Bulfares Section.

The volume augmentation produced by transformation of anhydrite to gypsum, leads fissures or hydration veins to be formed. These hydration veins are filled generally with satin-spar gypsum (Shearman *et al.,* 1972). The satin-spar gypsum indicates telogenetic alteration and secondary evaporite texture (Warren, 2016). This type of gypsum was recorded only in Nayab and Abgarmak Sections with a few mm thicknesses.

In some sections nodular texture was observed in both anhydrite and native sulphur mineral.

The nodular texture of anhydrite observed only in the Abgarmak Section. This nodular is surrounded by secondary gypsum. This suggests that it is deposited under synsedimentary condition and can be regarded as primary. The diameter of these nodules ranges between 6 cm and 14 cm (Fig. 6C).The nodular texture of native sulphur is found within the secondary gypsum matrix. The length of these nodules ranges between 1cm and 4cm (Fig. 6D).

Textures of gypsum can be regarded as near surface diagenetic (telogenetic) mechanisms and processes (Warren, 2016). Dissolution features are observed on the outcrops that are karren-like features (Fig. 7) (Madonia & Sauro, 2009). These features are mostly controlled by the water flowing above the rocky surfaces (Macaluso and Sauro, 1996a), include runnels and minute rills and are oriented according to the slope on a surface in alabastrine gypsum in all sections (Fig. 7A). Polygon pans are also present on gypsum outcrops which were formed by selective solution (Fig. 7B).

*Microscopic texture*
In this study petrographic assessments of evaporites found in the Asmari Formation show that the secondary gypsum has been produced by hydration of anhydrite during exhumation near-surface environment. The textures were altered during the deformation and recrystalization. Therefore, this gypsum could be interpreted as a part of diagenetic products.
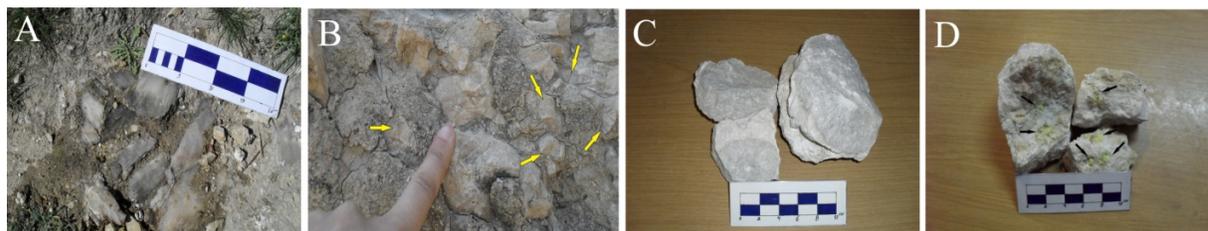


Figure 6. Secondary gypsum in the hand specimen and associated facies. (A-B) Fabrics of palisade and daisy gypsum within facies of secondary gypsum; A) Palisade gypsum, B) Daisy gypsum (arrows). C) Cut specimen of the anhydrite nodule (gray): the nodules are totally surrounded by secondary gypsum (white rim). D) Secondary gypsum hosting native sulphur nodules (arrows).
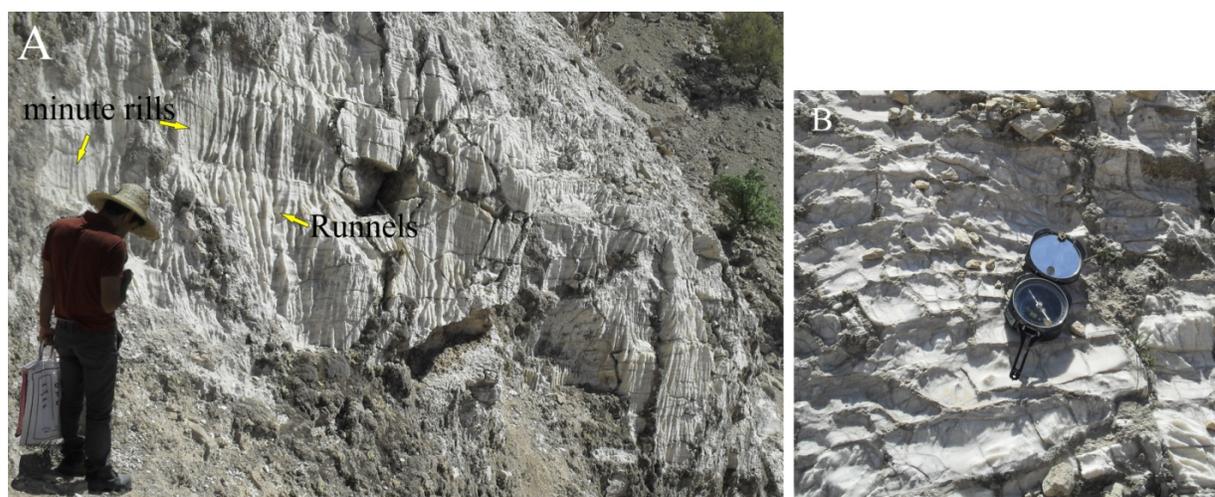
Figure 7. Different types of karren developed on alabastrine gypsum. A) Minute rills and runnels developed on steep surfaces of gypsum (Angarmak Section). B) Polygon pans evolved by selective solution on a surface of gypsum.

Petrographical properties of the secondary gypsum include: characteristics of crystalline textures, presence of microscopic relics of anhydrite and pseudomorphs after precursor anhydrite crystals (Ortí & Rosell, 2000).

Three different textures of the secondary gypsum were identified in the present study: alabastrine, porphyroblastic and fibrous. Secondary gypsum displayed densely-packed alabastrine and porphyroblastic textures that are associated mainly with relics of anhydrite.

Alabastrine or the microcrystalline texture contained xenotopic to idiotopic crystals. This texture included fine-grained crystals, in general <100μm in size, and a wide variety of related textures. Also, the contacts of fine crystals were usually irregular. Ortí *et al.,* (2010) recognized three main types of alabastrine textures, but in the present study only granular and prismatic textures have been observed in the thin sections.

Porphyroblastic or coarse-crystalline texture included anhedral and euhedral crystals. The coarse anhedral crystals had irregular boundaries. In some cases individual crystals were hard to define. This situation reveals the development of pseudomorphs of gypsum after anhydrite and according to Ciarapica *et al.,* (1985) and Testa and Lugli (2000) can be assumed as cloudy ameboid texture (Fig. 8A and 8G).

Each ameboid area showed undulose or irregular extinction under microscope (or in CPL). This type of texture includes abundant relics and corroded grains of anhydrite. Previous studies showed that the existence of relics and corroded grains of anhydrite are the signs of early product of anhydrite hydration and early diagenesis (Ogniben, 1957; Murray, 1964; Holliday, 1970; Ciarapica *et al.,* 1985; Testa & Lugli, 2000).

The microscopic studies showed that the coarse crystalline subhedral and euhedral texture formed large crystals interlocking structures at their margins and clearly defined individual crystals. These crystals occurred either single or as aggregates. The contacts between crystals were usually planar and polygonal (Fig. 8B). Moreover, euhedral and subhedral crystals showed sharp and uniform optical extinction. There were no quantities of anhydrite relics in this texture.

Fibrous texture observed in the thin sections of this study. They are pseudomorphs of secondary gypsum after anhydrite which includes daisy (rosette) (Fig. 8C), palmettos (Fig. 8D) and dendrite textures. Fibrous crystals had different sizes from 200μm to 400μm length in the thin section. In fact, this texture can be considered as coarse-crystalline texture. Petrographically, diagenetic gypsum also consisted of fibrous texture that in some cases reached up to 400μm length in the thin section and normally made up of satin-spar gypsum. They grew within fractures and veins and were recorded more or less in all the sections. The veins cut gypsum groundmass (Fig. 8E and 8H). Anhydrite relics present in coarse-crystalline (megacrystalline) texture of secondary gypsum due to conversion of anhydrite to gypsum (Fig. 8F).

In the studied sections, anhydrite and celestite were seen as well as secondary gypsum. Laths of anhydrite are observed as radial (especially daisy or

rosette-like) or fan-shaped in Abgarmak and Bulfares Sections. Rosette-like anhydrite revealed that the lathes are precursor of secondary gypsum or pseudomorphs of anhydrite (Fig. 9A and 9C).

Anhydrite relics were mainly present in the porphyroblastic and to a lesser extent in the alabastrine textures. These findings are consistent with Ortí *et al.,* 2011.
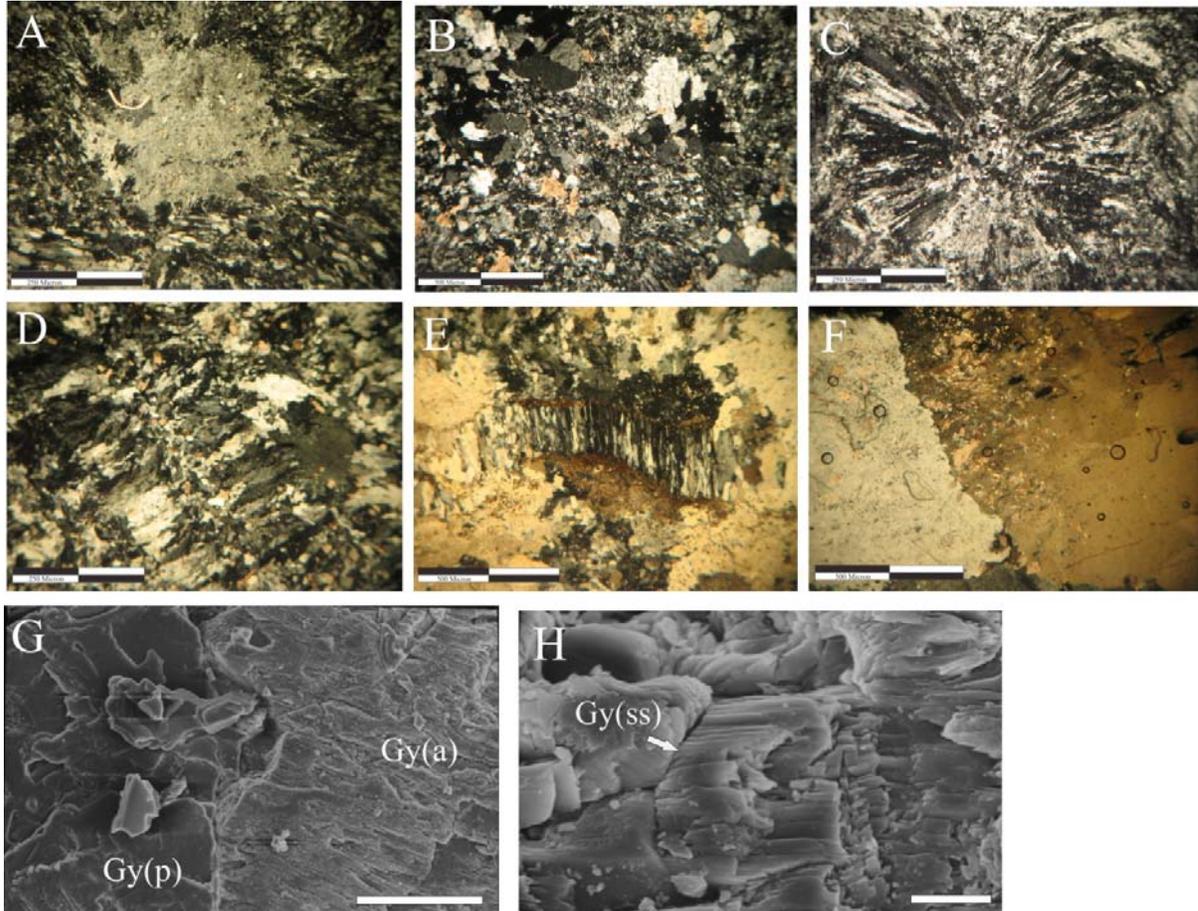


Figure 8. Textures of secondary gypsum from the Basal Anhydrite exposed in the study areas: A) Coarsely–crystalline anhedral (ameboid) texture, which has irregular crystal boundaries, undulose optical extinction and anhydrite relics. B) coarsely–crystalline euhedral show a sharp optical extinction and no anhydrite relics are present. C) and D) These pseudomorphs have a fibrous texture that preserves daisy (rosette)and palmettos textures, Respectively. These textures are derived from the hydration of precursor anhydrite during exhumation. E) The black and white fibrous visible in the center (vein) of the thin section are satin spar gypsum. F) Photomicrograph of Coarse-crystalline (megacrystalline) texture of secondary gypsum bearing anhydrite relics. G) SEM image of ameboid gypsum (Gy(a)) and porphyroblast gypsum (Gy(p)), bars: 100µm. H) SEM image of satin spar gypsum fibrous (Gy(ss)); bars: 10µm.
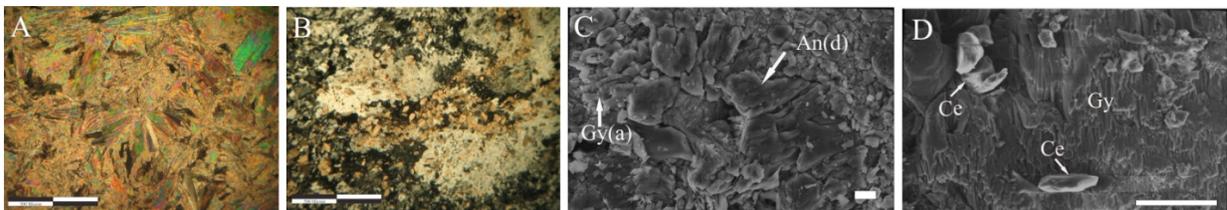


Figure 9. Textures of anhydrite and celestite. A) Fibrous anhydrite texture (daisy shape) B) Photomicrograph in cross-polarized light of a prismatic crystal of celestite. Photomicrograph in cross-polarized light of a prismatic crystal of celestite. C) SEM image of the daisy anhydrite (An(d)) as precursor alabastrine gypsum (Gy(a)). Scale: 10µm. D) SEM image of ameboid gypsum (Gy) and celestite (Ce); scale: 100µm. This material was depicted in figure 11B.

Small crystals of celestite usually accompany with the primary and secondary gypsum textures (Taberner *et al.*, 2002; Kasprzyk, 2003; Ortí *et al.*, 2011). In the studied thin sections, observed celestite crystals were found with secondary gypsum in place of conversion of anhydrite to gypsum. Therefore the existence of theses celestite crystals can be considered as a result of diagenetic process.

The celestite crystals mainly have microcrystalline shapes and appear in simple or aggregates forms. They are smaller than 100µm and found mostly with alabastrine secondary gypsum (Fig. 9B and 9D).

*The effect of tectonic on evaporite secondary texture:* the tectonic effect is mostly reflected in the textures that have been grouped in textures of dynamic and shock metamorphism in the metamorphic samples (Spry, 2013). This type of texture has been observed in evaporite deposits and due to its difference with metamorphic textures; it can be called "dynamic texture".

Besides three distinguished textures, the dynamic textures were also observed in thin sections in this study. The dynamic texture includes augen texture. This texture is visible in a part of the Abgarmak Section, where layers are inverted (Fig. 10A). The augen texture has cloudy ameboid gypsum and aligned-flowing gypsum. Ameboid gypsums are medium to coarse in size, with characteristic lenticular gypsum porphyroblasts. The matrix has fine to medium crystals and usually exhibits a parallel alignment of gypsum. In fact, the ameboid gypsum is warped by aligning gypsum (Fig. 10B) and texture in some thin sections displays bioturbation texture that can be the result of tectonic action in the area (Fig. 10C).

Bioturbation texture was observed in all sections due to the plastic nature of the evaporites. However augen texture and aligned-flowing gypsum have been seen only in the Abgarmak Section. Two types of porphyroblast textures were identified in the augen texture. *(1)Porphyroblast texture after hydration of anhydrite:* first stage, ameboid gypsum belongs to an earlier phase of hydration anhydrite (early diagenesis) (Ciarapica *et al.,* 1985; Testa & Lugli, 2000), which is surrounded by alabastrine secondary gypsum. Their formation criteria are similar to those given for coarsely crystalline anhedral crystal and alabastrine texture. At the next stage, alabastrine gypsum crystals may be recrystallized, and later form the coarse crystal gypsum (Urai *et al.* 1986). These phenomena are as a result of fine crystal conversion to coarse crystal through the diagenetic process which is affected by the deformation conditions (i.e. temperature) (Drury and Urai, 1990; Schenk and Urai, 2004). *(2) Porphyroblast texture as a result of tectonic activity:* At this stage, the ameboid gypsums are surrounded by aligned-flowing secondary gypsum and crystals were homogeneously oriented.
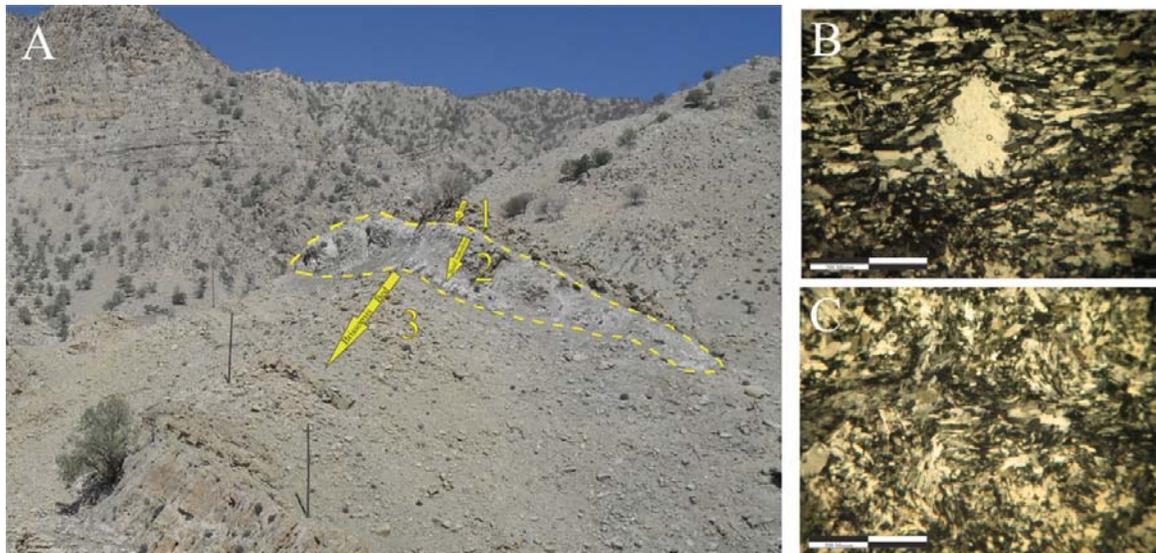


Figure 10. Inverted facies and typical textures of dynamic texture: A) Abgarmak outcrop section with inverted layers (from the base upward: 3: Brispossis Bed, 2: Basal Anhydrite, 1: Stromatolitic Boundstone). B) Augentexture: Coarse gypsum crystals that can be ascribed to recrystallization are present at the surrounding of the ameboid gypsum. C) Bioturbation texture.

The aligned-flowing gypsum is the result of recrystallization alabastrine gypsum that is influenced by tectonic process. This phenomenon eventually leads to the formation of porphyroblastic texture at the matrix. Thus, this texture is the result of later diagenetic association with tectonic movement (tectonic deformation) (Urai *et al.,* 1986, 2008).

## Conclusions

The Basal Anhydrite is observed at the base of the Asmari Formation and was replaced by secondary gypsum upon exhumation. Secondary gypsum is formed by ground water circulation or weathering of the calcium-sulphate.

Petrographical studies allow for differentiating between three types of gypsum textures: (1) Alabastrine and porphyroblast textures: They display pseudomorphic features inherited from the precursor anhydrite. Gypsum derived from hydration of anhydrite. (2) Fibrous texture: this texture has been formed as a result of precipitation from fluids of dissolved evaporates. (3) Dynamic texture: former gypsum and texture become deformed by tectonic processes.

Moreover, two textures are distinguished in nodules: (1) porphyroblastic texture: the outer zone of the native sulphur nodule (dark rim) is coarse-crystalline euhedral secondary gypsum with abundant anhydrite relics. Diagenetic celestite form porphyroblastic texture at the nodular boundary and display colors from beige to brown or gray. (2) alabastrine texture: this texture is surrounded by porphyroblast texture and includes chert-like and the microgranular type of alabastrin texture. Generally, the average size of crystals increases toward the center part (such as native sulphur).

The important result of this paper is the formation of the dynamic texture in the secondary gypsum based on tectonic processes. These processes have different tectonic effects due to the type of gypsum texture.

Dynamic texture includes aligned – flowing and augen texture. In the augen texture ameboid gypsum is surrounded by aligned – flowing texture. It is observed that ameboid gypsum was not deformed but alabastrine gypsum was deformed. Therefore, it can be concluded that most ameboid gypsums (or relic anhydrite-bearing gypsum) are more resistant against tectonic process in comparison with the alabastrine gypsum (or gypsums without relic).

## Acknowledgments

## References

Adams, T., 1969.The Asmari formation of Lurestan and Khuzestan provinces. Iranian Oil Operating Companies, Geological and Exploration Division, Report no. 1154 pp.

Adams, T., Bourgeois, F., 1967. Asmari Biostratigraphy. Iranian Oil Operating Companies, Geological and Exploration Division, Report no.1074 pp.

Ala, M.A., 1982. Chronology of Trap Formation and Migration of Hydrocarbons in the Zagros Sector of Southwest Iran. American Association of Petroleum Geologists Bulletin, 66: 1535-1541.

Aref, M. A. M., 1998b, Biogenic carbonates – are they a criterion for underlying hydrocarbon accumulations – an example from the Gulf of Suez region. American Association Petroleum Geologists – Bulletin, 82: 336–352.

Arzaghi, S., Khosrow-Tehrani, K., Afghah, M., 2012. Sedimentology and petrography of Paleocene-Eocene evaporites: the Sachun Formation, Zagros Basin, Iran. Carbonates and Evaporites, 27: 43–53.

Bąbel, M., 2004a .Models for evaporite, selenite and gypsum microbialite deposition in ancient saline basins. Acta Geologica Polonica, 54: 219–249.

Bąbel, M., 2007.Depositional environments of a salina-type evaporite basin recorded in the Badenian gypsum facies in the northern Carpathian Foredeep. In B. C. Schreiber, S. Lugli, M. Bąbel, Evaporites through Space and Time (pp. 107-142). Geological Society, London, Special Publications, 285 pp.

Carlson, E.H., 1987. Celestite replacements of evaporates in the salina group. Sedimentary Geology, 54: 93-112.

Ciarapica, G., Passeri, L., Schreiber, B.C., 1985. Una proposta di classificazione delle evaporiti solfatiche.. Geol. Rom, 24: 219–232.

Daraei, M., Amini, A.H., Ansari, M., 2014. Facies analysis and depositional environment study of the mixed carbonate–evaporite Asmari Formation (Oligo-Miocene) in the sequence stratigraphic framework, NW Zagros, Iran. Carbonates and Evaporites 30, no. 3: 253-272.

Dean, W.E., 1978. Trace of minor elements in evaporites. In: Dean, W.E., Schreiber, B.C. (Eds.), Marine Evaporites. SEPM Short Course, 4: 86–104.

Dronkert, H., 1985. Evaporite models and sedimentology of Messinian and Recent evaporites. GUA Papers of Geology, Ser. 1, No. 24: 1–283. Utrecht: GUA.

Drury, M.R., Urai, J.L., 1990. Deformation-related recrystallization processes. Tectonophysics, 172: 235–253.

Ehrenberg, S.N., Pickard, N.A.H., Laursen, G.V., Monibi, S., Mossadegh, Z.K., Svana, T.A., Aqrawi, A.A.M., Holliday, D.W., 1970. The petrology of secondary gypsum rocks.A review. Journal of Sedimentary Petrology 40: 734–744.

Holster, W.T., 1992. Stable isotope geochemistry of sulfate and chloride rocks. Lecture Notes in Earth Sciences, 43: 153-176.

Ingerson, E., 1968. Deposition and geochemistry work sessions. In: Mattox RB, et al. (ed.) Saline Deposits, New York: The Geological Society of America. Special Paper, 88: 671–681.

James, G.A., Wynd, J.G., 1965. Stratigraphic nomenclature of Iranian Oil Consortium Agreement Area. AAPG Bull, 49(12): 2182–2245.

Kavoosi, M.A., Sherkati, Sh., 2010. Depositional environments of the Lower Miocene evaporites of the Kalhur Member in the Zagros fold–thrust-belt, SW Iran. In: Abstracts of Proceeding of the 63th Geological Kurutali of Turkey, MTA-Ankara.

Kavoosi, M.A., Sherkati, Sh., 2012. Depositional environments of the Kalhur Member evaporites and tectonosedimentary evolution of the Zagros fold–thrust belt during Early Miocene in south westernmost of Iran. Carbonates and Evaporites, 27: 55-69.

Kinsman, D.J.J., 1966. Gypsum and anhydrite of recent age, Trucial Coast, Persian Gulf. Proc. 2nd Salt Symp., Northern Ohio Geol. Soc., 1: 302–326.

Macaluso, T., Sauro, U., 1996. Weathering crust and karren on exposed gypsum surfaces. International journal of speleology 25, 3-4: 115-126.

Madonia, G., Sauro, U., 2009. The karren landscapes in the evaporitic rocks of Sicily. In A. Ginés, M. Knez, T. Slabe, W. Dreybrodt (a cura di), Karst rock features – karren sculpturing (pp. 525-533). LJUBLJANA: Zalozba ZRC, ZRC SAZU.

Motiei, H., 1993. Stratigraphy of Zagros. Treatise on the Geology of Iran No. 1, Ministry of Mines and Metals, Tehran, Geological Survey of Iran.536 pp.

Motiei, H., 2001. Simplified table of rock units in southwest Iran. Tehran, Keyhan Exploration and Production Services.

Murray, R.C., 1964. Origin and diagenesis of gypsum and anhydrite. J. Sediment. Petrol. 34, 512–523.

Ogniben, L., 1957. Petrografia della Serie Solfifera Siciliana e considerazioni geologiche relative. Mem. Descr. Carta Geol. Ital. 33: 275 pp.

Ortí, F., Rosell, L., 2000. Evaporative systems and diagenetic patterns in the Calatayud Basin (Miocene, central Spain). Sedimentology, 47: 665-685.

Ortí, F., Rosell, L., Anadón, P., 2010. Diagenetic gypsum related to sulfur deposits in evaporates (Libros Gypsum, Miocene, NE Spain). Sedimentary Geology, 228: 304–318.

Ortí, F., Rosell, L., Playá, E., Salvany, J.M., 2011. Meganodular anhydritization: a new mechanism of gypsum to anhydrite conversion (Palaeogene–Neogene, Ebro Basin, North-east Spain). Sedimentology, 59: 1-21.

Ortí, F., Rosell, L., Playá, E., Salvany, J.M., 2012. Meganodular anhydritization a new mechanism of gypsum to anhydrite conversion (Palaeogene-Neogene, Ebro Basin, North-east Spain). Sedimentology, 59: 1257–1277.

Playá, E., Rosell, L., 2005. The celestite problem in gypsum Sr geochemistry: An evaluation of purifying methods of gypsiferous samples. Chemical Geology, 221: 102– 116.

Rahmani, A., A., Taheri, H., Vaziri-Moghaddam, A., Ghabeishavi, 2012. Biostratigraphy of the Asmari Formation at Khaviz and Bangestan Anticlines, Zagros Basin, SW Iran. Neues Jahrbuch für Geologie und Paläontologie-Abhandungen, 263 (1): 1– 16.

Schenk, O., Urai, J. L., 2004. Microstructural evolution and grain boundary structure during static recrystallization in synthetic polycrystals of sodium chloride containing saturated brine. Contributions to Mineralogy and Petrology, 146: 671–682.

Shearman, D.J., 1985. Syndepositional and late diagenetic alteration of primary gypsum to anhydrite. In: Schreiber, B.C., Harner, H.L. (Eds.), Sixth International Symposium on Salt. Salt Institute, 1: 41–50.

Shearman, D.J., Mossop, G., Dunsmore, H., Martin, H., 1972. Origin of gypsum veins by hydraulic fracture. Trans. Inst. Min. Metall. (Sect. B, Appl. Earth Sci.), 81: 149–155.

Spry, A., 2013. Metamorphic Textures. Elsevier Science. 358 pp.

Testa, G., Lugli, S., 2000. Gypsum–anhydrite transformations in Messinian evaporites of central Tuscany (Italy). Sedimentary Geology, 130: 249–268.

Urai, J. L., Spiers, C. J., Zwart, H. J., Lister, G. S., 1986. Weakening of rock salt by water during long-term creep. Nature, 324: 554–557.

Urai, J. L., Schléder, Z. Spiers, C. J., Kukla, P. A., 2008. Flow and Transport Properties of Salt Rocks. In: Littke, R., Bayer, U., Gajewski, D. Nelskamp, S. (Eds.). Dynamics of complex intracontinental basins: The Central European

Basin System. Springer- Verlag, Berlin Heidelberg, 277–290.

Van Buchem, F.S.P., Allan, T.L., Laursen, G.V., Lotfpour, M., Moallemi, A., Monibi, S.,  Motiei, H., Pickard, N. A.H., Tahmasbi, A.R., Vedrenne, V., Vincent, B., 2010. Regional stratigraphic architecture and reservoir types of the Oligo-Miocene deposits in the Dezful Embayment (Asmari and Pabdeh Formations) SW Iran. Geological Society, London, Special Publications, 329: 219-263.

Warren, J. K., 1999. Evaporites: Their evolution and economics. Oxford, UK, Blackwell Scientifi c, 438 p.

Warren, J. K., 2007. Evaporites: Sediments, Resources and Hydrocarbons. Berlin, Springer, 1041 pp.

Warren, J. K., 2016. Evaporites: A Geological Compendium. London, Springer, 1822 pp.

Warren, J. K., Havholm, K. G., Rosen, M. R., Parsley, M. J., 1990. Evolution of gypsum karst in the Kirschberg Evaporite Member near Fredericksburg, Texas. Journal of Sedimentary Petrology, 60: 721–734.